Geophysical Research Letters

RESEARCH LETTER
10.1029/2022GL102127

Key Points:

- Heterogeneous electrochemistry induced by Mars dust activity can decompose chloride, form (per) chlorate, carbonate, and release chlorine
- This experimental study simulated mid-strength Mars dust events and revealed the high yields of (per) chlorates, carbonates, and chlorine
- A calculation based on the results supports Martian dust activity as the major driving force for the global Cl-cycle in Amazonian period

Supporting Information:

Supporting Information may be found in the online version of this article.

Correspondence to:

A. Wang,
alianw@levee.wustl.edu

Citation:

Wang, A., Jackson, A. W., Sturchio, N. C., Houghton, J., Yan, C. Y. C., Olsen, K. S., & Qu, Q. H. K. (2023). Quantification of carbonates, oxychlorines, and chlorine generated by heterogeneous electrochemistry induced by Martian dust activity. *Geophysical Research Letters*, *50*, e2022GL102127. https://doi.org/10.1029/2022GL102127

Received 21 NOV 2022
Accepted 13 JAN 2023

Author Contributions:

Conceptualization: Alian Wang
Data curation: Alian Wang, Andrew W. Jackson, Neil C. Sturchio, Jen Houghton, Chuck Y. C. Yan, Quincy H. K. Qu
Formal analysis: Alian Wang, Andrew W. Jackson, Neil C. Sturchio, Jen Houghton, Chuck Y. C. Yan, Quincy H. K. Qu
Funding acquisition: Alian Wang, Andrew W. Jackson, Neil C. Sturchio

Quantification of Carbonates, Oxychlorines, and Chlorine Generated by Heterogeneous Electrochemistry Induced by Martian Dust Activity

Alian Wang[1], Andrew W. Jackson[2], Neil C. Sturchio[3], Jen Houghton[1], Chuck Y. C. Yan[1], Kevin S. Olsen[4], and Quincy H. K. Qu[1]

[1]Department Earth & Planetary Sciences and McDonnell Center for the Space Sciences, Washington University in St. Louis, St. Louis, MO, USA, [2]Department Civil, Environmental, and Construction Engineering, Texas Tech University, Lubbock, TX, USA, [3]Department Earth Sciences, University of Delaware, Newark, DE, USA, [4]Department Physics, Oxford University, Oxford, UK

Abstract Heterogeneous electrochemistry induced by Martian dust activity is an important type of atmosphere-surface interaction that affects geochemical processes at the Martian surface and in the Martian atmosphere. We have experimentally demonstrated that heterogeneous electrochemistry stimulated by mid-strength dust events can decompose common chloride salts, which is accompanied by the release of chlorine atoms into the atmosphere and the generation of (per)chlorates (chlorates and perchlorates) and carbonates. In this study, we present quantitative analyses on the above products from 26 heterogeneous electrochemical experiments on chloride salts. Based on these quantifications, our calculation indicates that such atmosphere-surface interaction during a portion of Amazonian period could accumulate the observed abundance of (per)chlorates, carbonates, and HCl by landed and orbital missions, and thus can be considered as a major driving force of the global chlorine-cycle on Mars. This study emphasizes the importance of measuring the electrical properties of dust activity on Mars.

Plain Language Summary Frictional electrification is a common process in our solar system, with Martian dust activities known to be a powerful source of electrical charge buildup. Furthermore, the thin atmosphere on Mars makes the breakdown of accumulated electrical fields, in form of electrostatic discharge (ESD), much easier to occur (a hundred times easier than on Earth). ESD generates a huge amount of energetic electrons that collide with Martian atmospheric molecules and generate free radicals. These free radicals react with the Martian chlorides to generate new species. This study found the yields of (per)chlorates, carbonates, and chlorine from the ESD process, with the strength matching mid-strength Martian dust activity, are at per thousand or percent levels (normalized to the starting chlorides). Based on these results, it is possible to calculate the total yields of those species produced from known chloride sources on Mars by global dust storms during defined durations in the Amazonian period. It was found that the contributions of Mars dust activity can account for the abundances of (per)chlorates, carbonates, and chlorine observed by past and current Mars missions. This study supports that Martian atmosphere-surface interaction in dust events is a major driving force for the global chlorine-cycle on Mars.

1. Introduction

Heterogeneous electrochemistry induced by Martian dust activity is an important type of atmosphere-surface interaction that could affect geochemical processes on the Martian surface and in the Martian atmosphere. However, there has been no actual measurement made of the electrical properties of Martian dust events, due to mission descope or failure. For that reason, simulating experiments for heterogeneous electrochemistry in form of electrostatic discharge (ESD) in Mars chambers and theoretical modeling are the common ways to study the chemical process that could be induced by Martian dust activities (Atreya et al., 2006; Bak et al., 2017; Delory et al., 2006; Farrell et al., 2015; Martínez-Pabello et al., 2019; Tennakone, 2016; A. Wang, Yan, Dyar, et al., 2020; A. Wang, Yan, Jolliff, et al., 2020; A. Wang et al., 2022; Wu et al., 2018).

We conducted 26 sets of ESD experiments on chloride salts in a Mars reaction chamber (Figure S1 and Table S1 in Supporting Information S1), with a range of electron flux densities that match those for mid-strength dust events on Mars (Figure S4d and Table S2 in Supporting Information S1). We selected two chlorides KCl and

Investigation: Alian Wang, Andrew W. Jackson, Neil C. Sturchio, Jen Houghton, Chuck Y. C. Yan, Kevin S. Olsen
Methodology: Alian Wang, Andrew W. Jackson, Neil C. Sturchio, Kevin S. Olsen
Project Administration: Alian Wang
Resources: Alian Wang
Supervision: Alian Wang
Validation: Alian Wang, Andrew W. Jackson, Neil C. Sturchio
Writing – original draft: Alian Wang, Andrew W. Jackson, Neil C. Sturchio
Writing – review & editing: Alian Wang, Andrew W. Jackson, Neil C. Sturchio, Jen Houghton, Chuck Y. C. Yan, Kevin S. Olsen, Quincy H. K. Qu

$MgCl_2$ for this study, to represent two groups of common chlorides (KCl, NaCl, and $CaCl_2$ vs. $MgCl_2$, $AlCl_3$, and $FeCl_2$) that demonstrated distinct behaviors in three aspects (Table S3 in Supporting Information S1).

This study emphasized on the quantification of the (per)chlorate, carbonate, and oxide in the post-ESD remaining salt, as well as Cl and ClO_x (x = 1–4) in the exhaust gas both directly and using solution traps (Figure 1). These quantifications built a basis to estimate the required time duration in Amazonian period (%) to generate the observed abundances of these species on Mars, by dust activities only. Sequential Ion Chromatography (IC)-mass spectroscopy-mass spectroscopy (IC-MS/MS), IC, Thermo-flash elemental analyzer, associated with the wet-chemical procedure, gas sensors, and in situ Raman, MIR spectroscopy, and XRD were used for characterization and quantification of reaction products (Figure 1).

This study revealed a complete set of products from the electrochemically induced decomposition of chlorides when impacted by energetic electrons under Mars's relevant atmospheric conditions. The quantifications approximately closed the mass balances of chlorine and cations. It revealed an overall picture of Cl, O, and C, transformation pathways in a major process, relevant to three of the five mobile elements (Cl, O, C, H, and S) on Mars.

2. Results

2.1. Identifications of Carbonate and (per)chlorates

Raman, FTIR-ATR, and powder XRD were selectively made on post-ESD remaining salts.

Almost every spectrum in a 50-spot micro-beam Raman scan on the product of 7hr-ESD-on-KCl (Figure 2a) shows the characteristic Raman ν_1 peaks of $KClO_3$ (938) and K_2CO_3 (1,052 cm^{-1}). Similarly, the characteristic mid-IR ν_3 peaks of $KClO_3$ (968 and 939) and K_2CO_3 (1,364 cm^{-1}) are observed from the same samples (Figure 2b). Similar type Raman ν_1 peaks that belong to M-CO_3 and M-ClO_3 (M = Na, Al, Ca) were also observed on the remaining salts of ESD-on-NaCl, -$CaCl_2$, and -$AlCl_3$ (Figure S2 in Supporting Information S1).

The typical Raman and MIR peaks of $Mg(ClO_3)_2$ and $MgCO_3$ were not seen from the remaining salts of 7hr-ESD-on-$MgCl_2$, perhaps due to their presence as amorphous forms because $MgCl_2$ was observed to become amorphous after 7 hr-ESD (A. Wang, Yan, Dyar, et al., 2020). XRD analyses of remaining salts of ESD-on-KCl and ESD-on-$MgCl_2$ showed no detection of chlorates or carbonates suggesting low concentrations (<1 mol%).

The formation rates of chlorates and carbonates are high, almost instantaneous. They are evidenced in the Raman spectra of the remaining salts from ESD-on-NaCl (Figure S3 in Supporting Information S1), by the appearance of ν_1 peak of $NaClO_3$ after only 15 min of ESD, and ν_1 peak of Na_2CO_3 after only 1 hr of ESD, respectively. $NaClO_4$ was also formed but at a much lower abundance (top spectrum in Figure S3 in Supporting Information S1).

2.2. Cl Distributions in Oxyanions (HOCl, ClO_2^-, ClO_3^-, ClO_4^-) and as Released Cl^-

Reaction products were evaluated in the post-ESD remaining salt, the Cl-bearing film deposited on electrodes, and the trapping solutions of exhaust gas (Figure 1). The latter two collectively represent the total gas-phase Cl produced, which was obtained by summing the molar masses of Cl in ClO_3^-, ClO_4^-, ClO_2^-, HOCl, and Cl^- in trapping solutions (#1 and #2) and the ClO_3^-, ClO_4^-, and Cl^- in solution #3 (dissolved Cl-bearing film on the electrode). The overall uncertainty in these analyses is ±20%.

Due to the production of free radicals and reactive gases (CO_2^+, CO^+, O_I, and O_3) during ESD in CO_2, we do not focus on the speciation of Cl in the solution traps because additional oxidation after trapping could have occurred. Rather we evaluate the total Cl in the gas phase as a measure of released Cl from chlorides, compared to the Cl in ClO_3^- and ClO_4^- in the post-ESD remaining salts. In Figure 3, these values are presented as a mol%, that is, the sum of Cl mole in products normalized to the total Cl mole in initial chlorides (KCl or $MgCl_2$).

Most of the reacted Cl was released in the gas phase, (≥1 mol%). In comparison, the Cl in M-ClO_3 and M-ClO_4 (M = K, Mg) in the remaining salts were much lower (*per thousand and per million*, respectively) (Figure 3a). The quantities Cl in oxyanion species in the exhaust gas decreased with the increase of Cl oxidation state, that is, 10^{-3}–10^{-4} in HOCl, 10^{-4}–10^{-5} in ClO_2^-, 10^{-5}–10^{-6} in ClO_3^-, and 10^{-10}–10^{-11} in ClO_4^- (Figure 3b).

In addition to analytical uncertainty, the major parameter that affects the fluctuation in the yields of released or oxidized Cl is the electron flux density (EFD) that varies during an ESD experiment and fluctuated among

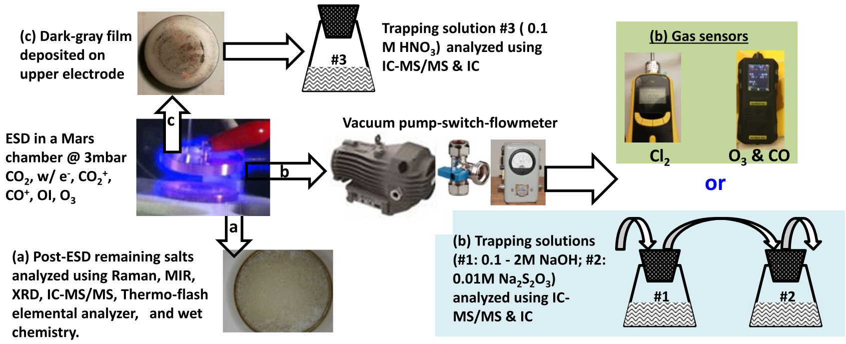

Figure 1. Products from ESD_on_KCl (or $MgCl_2$) in a Mars reaction chamber: (a) Post-electrostatic discharge remaining salts; (b) Exhaust gas; (c) Dark-gray film deposited on upper electrode. The characterization and quantification were made using Raman, MIR, XRD, IC-MS/MS, Ion Chromatography, Thermo-flash elemental analyzer, wet chemistry, and gas sensors.

the 17 ESD experiments whose products were analyzed here (Figure S4 in Supporting Information S1). Overall, we obtained the mean value and standard deviation of Cl in ClO_3^- + ClO_4^- in the remaining salts to be 0.07 ± 0.04 mol% and those for released gaseous Cl to be 1.1 ± 0.9 mol%. Consistent with our previous observation on the cation effect (Table S3 in Supporting Information S1), the mean yield of ClO_3^- + ClO_4^- in remaining salts from ESD-on-KCl (0.09 ± 0.04 mol%) is slightly higher than that from ESD-on-$MgCl_2$ (0.04 ± 0.03 mol%); while the mean released Cl from ESD-on-KCl (0.9 ± 0.8 mol%) is slightly lower than that from $MgCl_2$ (1.3 ± 0.9 mol%).

2.3. Additional Detection of the Released Cl

In addition to measuring the Cl-bearing film and Cl in trapping solutions, we quantified Cl_2 gas directly in the exhaust gas line (after a flow meter), either after the trapping solutions or without them (Figure S1 in Supporting Information S1). Figure 4a compares the Cl_2 readings, Figure 4b compares the CO and O_3 readings (Figure S5 in Supporting Information S1 shows the change of gas sensor reading during a 7hr-ESD experiment). These results (a) confirm a large amount of Cl_2 was released in the exhaust gas line, (supporting the phase analysis of trapping solutions) and (b) show a reduction of gas flow rate (Figure 4a) in the system when the solution traps were connected. The gas flow rate can affect the film deposition onto the electrodes, thus we do not seek to build a quantitative relation from the Cl_2 sensor reading to the Cl in trapping solutions determined by IC-MS/MS.

Nevertheless, a good match was found between the Cl trapped in the solutions (Figure 3a) and the gravimetric measurement of Cl in the deposited films on electrodes (Figure S6 in Supporting Information S1) after they were removed and weighed (Table S4 in Supporting Information S1). Both are at *the percent level*.

2.4. Total Carbon Analysis and Carbonate Concentrations

The remaining salts from four ESD experiments (two ESD-on-KCl and two ESD-on-$MgCl_2$, Table S1 in Supporting Information S1) were used for this analysis. Multiple aliquots of each of two replicate experimental sets of remaining salts were measured for total carbon content by quantification of the amount of CO_2 released into a helium carrier gas stream with combustion at 1000°C in an elemental analyzer.

The results of these analyses indicated that the total amount of carbon in the remaining salts of ESD-on-$MgCl_2$ was 0.47 μg C per milligram salt (or ∼0.37 mol% $MgCO_3$), whereas that in the remaining salts of ESD-on-KCl was 0.23 μg C per milligram salt (or ∼0.29 mol% K_2CO_3) (Table 1). Uncertainties of these values exceed those of the calibration data set (relative standard deviation ±10% over the range of calibration, Figure S7 in Supporting Information S1), likely indicating substantial heterogeneity of the remaining salts at the scale of the analyzed aliquots (4–21 mg). Nonetheless, the total carbon results are consistent with the presence of small amounts of carbonate minerals (Figure 2), an average of ∼0.33 mol% of cation in the initial chloride taken by carbonates, produced by the reaction of CO_2 and its electrolysis products with chloride salts under the Mars-like atmospheric conditions.

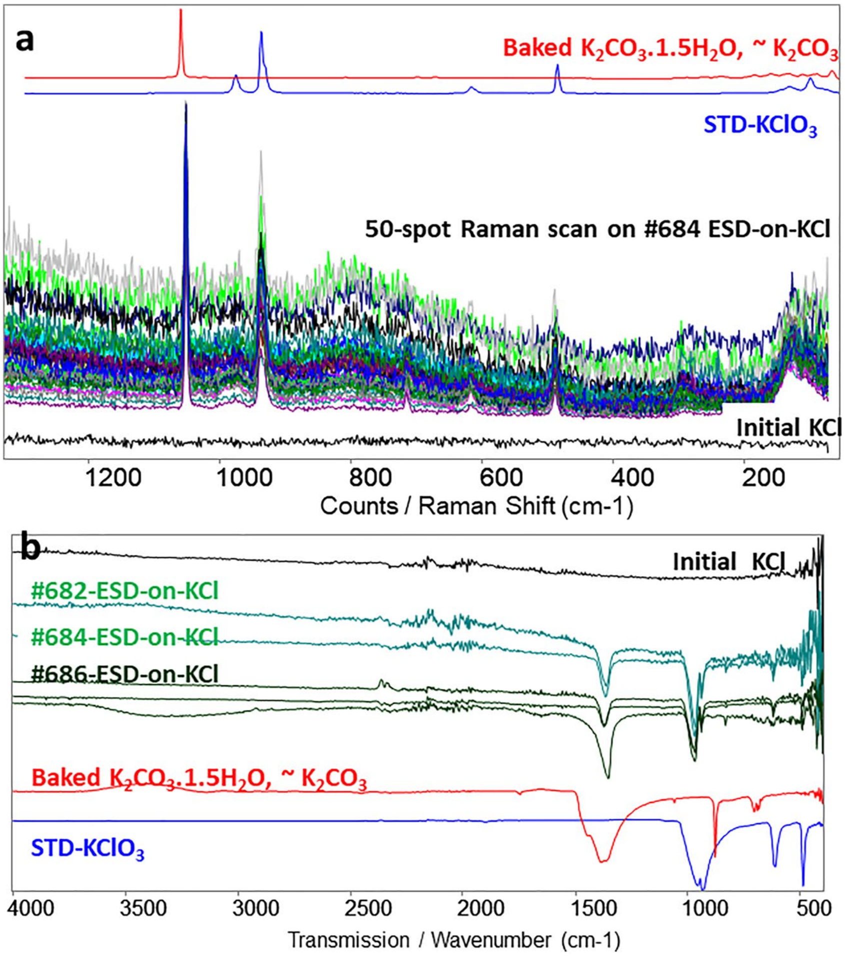

Figure 2. Raman and MIR spectra of initial chloride, electrostatic discharge (ESD) products, and standards. (a) The Raman peak positions of ESD-generated $KClO_3$ shows a perfect match with a pure $KClO_3$ chemical (XRD confirmed), while that of ESD-generated K_2CO_3 has a slightly shifted ν_1 peak from that of a pure K_2CO_3 chemical (Sigma-Aldrich, batch#09707CE) which was identified as $K_2CO_3 \cdot 1.5H_2O$ by XRD. The discrepancy does not disappear after it was baked at 220°C overnight for unknown reason. A potential interpretation based on a past Raman spectroscopic study of K_2CO_3 and $KHCO_3$ at high temperature and high pressure (Frantz, 1998), which suggested that the Raman ν_1 peak position shifts to lower wavenumber (from 1,072 to 1,048 cm^{-1}) might occur following a temperature increase (from 24°C to 548°C). (b) The MIR peak positions of ESD-generated $KClO_3$ shows a perfect match with a pure $KClO_3$ chemical (XRD confirmed), while that of ESD-generated K_2CO_3 has a single narrow ν_3 peak, but the baked $K_2CO_3 \cdot 1.5H_2O$ shows a much wide and multi-component ν_3 peak that can be caused by site-group-splitting. The loss of spectral details in the spectrum of ESD-generated K_2CO_3 can be caused by a lower crystallinity when it formed at higher temperature in ESD process.

2.5. Identification and Quantification of Oxides

A large amount of Cl release suggests the decomposition of original chloride molecules. Some of the liberated cations (K^+ or Mg^{2+}) went into (per)chlorates, some went into carbonates. However, some remaining liberated cations must have gone into an additional molecular form.

We hypothesize that some oxides (MgO or K_2O) were formed, although these oxides were not seen in Raman and MIR spectra because they have Raman/MIR cross sections smaller than those of ClO_3^- or CO_3^{2-}; nor were they detected by XRD. However, water-insoluble residues were observed when analyzing the remaining salts of ESD-on-$MgCl_2$ but not that of ESD-on-KCl, which suggested the formation of $Mg(OH)_2$ (solubility ~ 0.00069 g/100 g H_2O for $Mg(OH)_2$, and ~121 g/100 g H_2O for KOH, Lide, 2001) by reaction of MgO with water.

To confirm this hypothesis, we rinsed chemically pure MgO with water and used XRD to confirm that the generated insoluble residue was >99% $Mg(OH)_2$ (Figure S8 in Supporting Information S1). Then we dissolved the

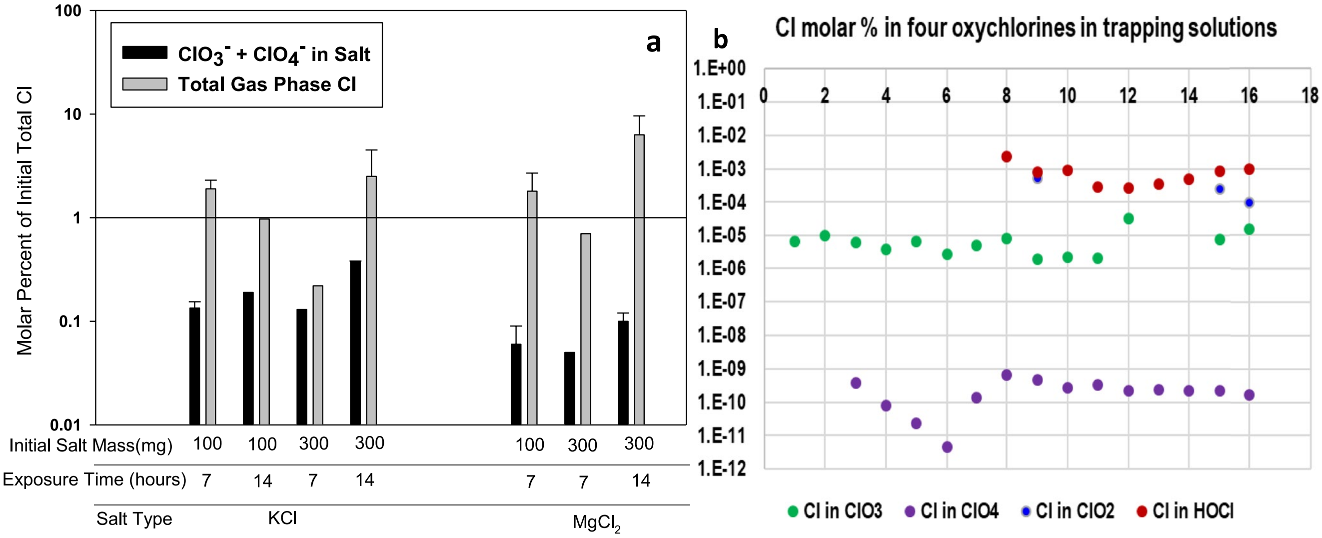

Figure 3. Cl distributions: (a) Cl in M-ClO_3 + M-ClO_4 (M = K or Mg) in the remaining salts, and released Cl in exhaust gas; (b) Cl in HOCl, ClO_2^-, ClO_3^-, and ClO_4^- in trapping solutions. Both plots show the molar ratio (%) normalized over the total Cl in initial chlorides (KCl or $MgCl_2$).

remaining salts from three ESD experiments on $MgCl_2$ (Table S1 in Supporting Information S1) and analyzed the insoluble residues using XRD which confirmed >99% of $Mg(OH)_2$, plus possible Mg_2C (Figure S8 in Supporting Information S1). Additional Raman and MIR spectra supported a hydroxide as the major phase of these insoluble residues. We carefully weighed the masses of residues (±0.001 mg) and the starting salts (±0.001 g), then calculated the molar ratio of Mg in $Mg(OH)_2$ against the total Mg in original $MgCl_2$. A range of 0.7–2.8 mol% was found for the insoluble residue of three ESD-on-$MgCl_2$ (Table 2).

This result supports that MgO is the molecular form of the remaining liberated Mg^{2+}, with a produced quantity that matches the released Cl, that is, both are *at the percent level*.

3. Discussion

3.1. Free Radicals, Electrochemical Reactions, and Mass Balance

Knowledge of available free radicals will help to understand electrochemical reactions occurred during the studied ESD process. The in situ plasma and UV spectra obtained during ESD (Figure S9 in Supporting Information S1) revealed that CO_2^+, CO^+, O_I, and O_3 are generated from ESD in dry CO_2. When using a simulated Mars gas mixture (CO_2, N_2, Ar, O_2, trace H_2O), additional free radicals, including Ar_I, N_2^*, N_2^+, H_{III}, H_{II}, OH^*, O_{II},

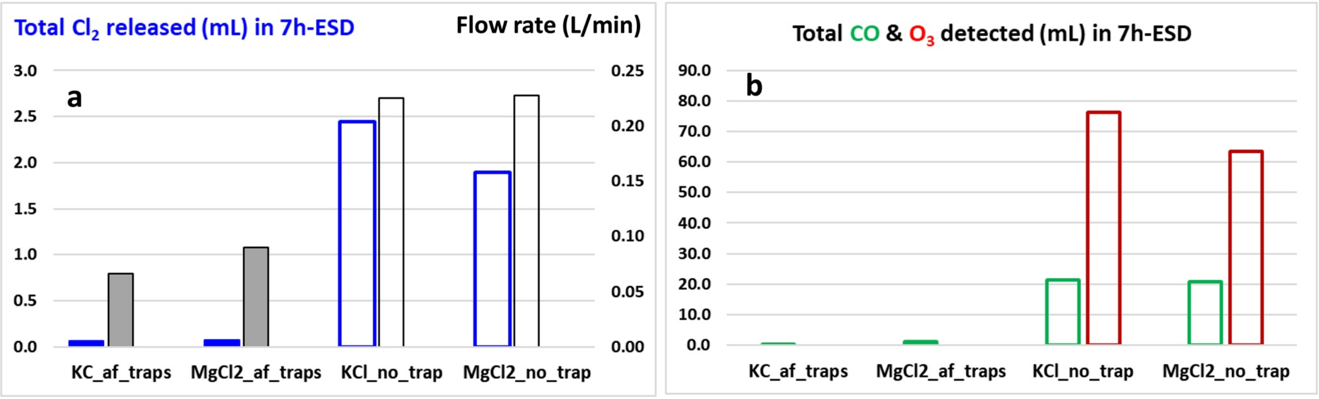

Figure 4. The gas sensor reading summed over 7 hr' electrostatic discharge (ESD) for four types of 13 ESD experiments: (a) Cl_2 (mL) and flow rate (L/min), (b) CO and O_3 (mL). The uncertainties of Cl_2 sensor, flow meter, and CO & O_3 sensor are ±3%, ±1%, ±10%, ±5%, respectively. Although some ESD experiments have lasted 14 hr, only the summed first 7 hr reading were compared here.

Table 1

Total Carbon Analyses Results and Carbonate Quantification as the Molar Ratio of Cation in Carbonates Normalized Over the Total Cation in Initial Chlorides

Sample ID	# Aliquots	µg C/mg	Std dev	Carbonates	Concentration (mole %)
#680 ESD-on-$MgCl_2$	8	0.47	0.23	$MgCO_3$	0.37%
#681 ESD-on-$MgCl_2$	7	0.47	0.42	$MgCO_3$	0.37%
#682 ESD-on-KCl	11	0.23	0.19	K_2CO_3	0.29%
#683 ESD-on-KCl	8	0.23	0.14	K_2CO_3	0.29%

and Ar_{II}, are available (Figure S9 in Supporting Information S1). These free radicals, plus primary and secondary electrons, with high chemical reactivity and high kinetic energy, would impact the top surface of the chloride salts, causing further reactions.

The results from our analysis of ESD products suggest that the following reactions must have occurred, where M = Mg or K:

$$e^- + \text{M-Cl} \quad \rightarrow \quad \text{Cl}_\text{I} + \text{M}^* \tag{1}$$

$$\text{Cl}_\text{I} + (\text{O}_\text{I}, \text{O}_\text{II}, \text{O}_3) + \text{M}^* \quad \rightarrow \quad \text{M-ClO}_3 \tag{2}$$

$$\text{M-ClO}_3 + (\text{O}_\text{I}, \text{O}_\text{II}, \text{O}_3) \quad \rightarrow \quad \text{M-ClO}_4 \tag{3}$$

$$\text{M}^* + (\text{O}_\text{I}, \text{O}_\text{II}, \text{O}_3) \quad \rightarrow \quad \text{M-O} \tag{4}$$

$$\text{M}^* + \left(\text{CO}_2{}^+, \text{CO}^+, \text{O}_\text{I}, \text{O}_\text{II}, \text{O}_3\right) \quad \rightarrow \quad \text{M-CO}_3 \tag{5}$$

The decomposition of chloride by energetic electrons (Equation 1) is a first-order reaction. It generates two products, the Cl_I and M* (Cl_I marks the first excited state of Cl atom, M* marks the excited cation, Mg or K) that appear as the released Cl^-/Cl_2 gas, and M-oxides (Equation 4). Within the experimental fluctuation range, the yields of Cl in released Cl^-/Cl_2 and of M in M-oxides are at the same level, that is, *the percent level* when normalized to the totals in initial chlorides. Therefore, the mass balances in Cl and in cations were approximately (in the orders of magnitude) closed. In addition, portions of these yields (i.e., at the *per thousand level* vs. the totals of initial chlorides) served as the starting species (Cl_I and M*) in the formation of chlorates (Equation 2) and carbonates (Equation 5). Furthermore, chlorate is sequentially oxidized to perchlorate (Equation 3) with a yield at the per thousand level (i.e., *at ppm level* vs. the totals of initial chlorides).

The quantifications of Cl in oxychlorine species (trapped by three solutions), especially the decreasing trend with the increasing oxidation state (Figure 3b), suggest the following sequential oxidations occurred, with gradually increased valence state of Cl from Cl^{+1} to Cl^{+3}, to Cl^{+5}, and to Cl^{+7}:

Table 2

Quantification of $Mg(OH)_2$ Mass, and Molar Ratio of Mg in MgO Normalized Over the Total Mg in Initial $MgCl_2$

			Assume $MgCl_2$ was the starting phase[a]	Assume $MgC_2·6H_2O$ was the starting phase[a]
Sample ID	Starting solid (g)	Ending solid (g) = $Mg(OH)_2$, ID by XRD, Raman, MIR	% of Mg in MgO versus Mg in starting phase[b]	% of Mg in MgO versus Mg in starting phase[b]
#685 ESD-on-$MgCl_2$	0.218	0.001772	1.3%	2.8%
#680 ESD-on-$MgCl_2$	0.125	0.000516	0.7%	1.4%
#681 ESD-on-$MgCl_2$	0.112	0.000465	0.7%	1.4%

[a] Because the actual starting phase may have moderate hydration, that is, in between of $MgCl_2$ and $MgCl_2·6H_2O$ (the stable Mg-chlorides in laboratory are $MgCl_2.2H_2O$, $MgCl_2.4H_2O$ or $MgCl_2.6H_2O$ depending on temperature and relative humidity, Shi et al., 2019), the final mol% Mg in $Mg(OH)_2$ (vs. starting salt) should be a middle value between 0.7% and 2.8% (stated in text). [b] When assuming all MgO was converted to $Mg(OH)_2$ in H_2O, and all $Mg(OH)_2$ was precipitated, the mole % Mg in MgO should be the same.

$$Cl_{I} + (O_{I}, O_{II}, O_3) \rightarrow HOCl \tag{6}$$

$$HOCl + (O_{I}, O_{II}, O_3) \rightarrow ClO_2^{-} \tag{7}$$

$$ClO_2^{-} + (O_{I}, O_{II}, O_3) \rightarrow ClO_3^{-} \tag{8}$$

$$ClO_3^{-} + (O_{I}, O_{II}, O_3) \rightarrow ClO_4^{-} \tag{9}$$

3.2. Scale to Mars From the Quantifications of This Study

We have quantified the yields (Figure 3, Tables 1 and 2) of (per)chlorates, carbonates, and Cl release from two typical chlorides after 7 hr ESD exposures that have an average EFD matching the mid-strength dust events on Mars (Table S2 in Supporting Information S1). Now we can link these yields with the observed abundances of relevant species on Mars, thus to understand the role of heterogeneous electrochemistry in driving the Martian chlorine-cycle.

A calculation (Table S5 in Supporting Information S1) was conducted. We used the mean values of three quantifications of this study (Table S5a in Supporting Information S1), the lowest end of available chloride sources on Mars (Table S5b in Supporting Information S1, Glotch et al., 2016; Osterloo et al., 2008, 2010), and the average temporal and areal coverage of global dust storms (GDS) on Mars (Table S5c in Supporting Information S1, H. Wang & Richardson, 2015), to find the duration (in %) of the Amazonian period that would be needed to reach the highest reported perchlorate abundances (Table S5d in Supporting Information S1, Hecht et al., 2009; Kounaves et al., 2010) and carbonate abundances (Table S5e in Supporting Information S1, Bandfield et al., 2003; Boynton et al., 2009; Christensen et al., 2004), considering only the effect of heterogeneous electrochemistry.

Only GDS were used in this calculation (Table S5c in Supporting Information S1). Other dust activities, for example, dust devils, regional dust storms, and grain saltation, can all stimulate ESD. However, quantifying their temporal and areal coverage to factor them into this calculation would be impossible; their effects were ignored here for simplification.

Two major assumptions were used in this calculation. First, 0.0001 was used as the ESD occurrence probability during GDS (Table S5c in Supporting Information S1), which was arbitrarily selected in an early study (A. Wang, Yan, Dyar, et al., 2020), but was retained to keep the consistency throughout our studies. A probability of 1–2 orders of magnitude higher is entirely possible, pending the real measurement of electrical properties of dust activities on Mars in the future, like the payloads prepared by Farrell et al. (2000) for NASA and Harrison et al. (2016) for ESA missions. Second, we used a very small chloride source area on Mars based on early publications (Glotch et al., 2016; Osterloo et al., 2008, 2010) as the starting point (Table S5b in Supporting Information S1). New observations have revealed a much higher number of chloride-bearing sites on Mars (Hill, 2022), and much higher (than 10% we used here) chloride abundance at many sites (Das et al., 2022).

Our calculation (Tables S5d and S5e in Supporting Information S1) shows that when considering only the contribution of heterogeneous electrochemistry (GDS only) with the lowest chloride source on Mars (area ratio ~0.0035%, 10% chloride concentration), the highest the observed abundance of ClO_4^{-} at 0.7 wt% and of carbonates at 5 wt% within the entire Martian topsoil can be accumulated after $\sim 4.6 \times 10^8$ and $\sim 7.0 \times 10^8$ Martian years, respectively. These time durations correspond to ~16% and ~24% of the Amazonian period. For simplification, this calculation does not include the (per)chlorates contributed by photochemistry (Carrier & Kounaves, 2015; Gure et al., 2019; Schuttlefield et al., 2011; Zhao et al., 2018), by galactic cosmic ray impact (Wilson et al., 2016), and the carbonates contributed by ground carbonate-bearing outcrops and distributed by aeolian processes.

We found the Cl released from chlorides is extremely high (average 1.1 mol%, Figure 3, Figure S4b, Table S4 in Supporting Information S1) during a 7 hr heterogeneous electrochemical experiments. In the calculation to scale this yield to observed HCl abundance in the atmosphere, a different approach was taken. Because the TGO observation was made during a single year on Mars (MY 34 or MY 35) and correlated with dusty seasons, the GDS contribution of a single Martian year from the whole Martian globe should be considered in the calculation. Since HCl has a lifetime of at least a few months (Aoki et al., 2021; Olsen et al., 2021), the accumulation of released Cl in a GDS-dust season is considered.

Assuming the thickness of lifted topsoil by a GDS to be 1–10 cm (a conservative estimation), we can get the total volume of ESD-affected chloride to be 4×10^{-7} km^3 (using 0.0035% ratio of the chloride-bearing area over the whole Martian surface as the low end, by Osterloo et al., 2008, and 10% chloride concentration, by Glotch et al., 2016) to 1.28×10^{-5} km (using the 0.011% area ratio as high end, Osterloo et al., 2010). When taking NaCl to represent the affected chlorides (Glotch et al., 2016), the total released number of Cl atoms is 2.32×10^{31} to 7.42×10^{32}. Assuming all Cl atoms reacted with H to form HCl (Catling et al., 2010), and the HCl molecules are distributed into the atmosphere below 40 km, the HCl number density would be in the range of 4.0×10^6 to 1.3×10^8 molecule/cm^3 (Table S5f in Supporting Information S1). This estimated range matches the observed range (2×10^6 to 2×10^8 molecule/cm^3) by the TGO mission (Figure S10c in Supporting Information S1, Korablev et al., 2021; Olsen et al., 2021). This match supports that the GDS stimulated heterogeneous electrochemistry releases enough chlorine into atmosphere (through decomposing the surface chlorides) as observed by mission. Therefore, it is the major driving force of the chlorine-cycle on Amazonian Mars (Figure S11 in Supporting Information S1).

In conclusion, our experiments revealed high yields of chlorine, (per)chlorates, and carbonates from simulated heterogeneous electrochemical processes whose electron flux densities match mid-strength Martian dust activities. A simple calculation based on these quantifications generated the results that match the observed abundances of HCl, (per)chlorates, and carbonates by missions to Mars. This study demonstrated that ESD-driven atmosphere-surface interaction can be a major contributor to many geochemical processes on the Martian surface and in its atmosphere. This study emphasizes, again, the importance of measuring the electrical property of dust activity in future missions to Mars.

Conflict of Interest

The authors declare no conflicts of interest relevant to this study.

Data Availability Statement

Supporting Information S1 document is submitted that includes the methods, figures, and tables. The digital data of all presented spectra and plots are included in an excel file. The Scale-to-Mars calculation is in a second excel file. Both are available at a permanent repository website managed by the library of Washington University in St. Louis, DOI: https://doi.org/10.7936/b3ps-em15, No user ID and password are required for the access of these data.

Acknowledgments
This work was funded by the NASA Solar System Working program, SSW-80NSSC17K-0776 and SSW-80NSSC21K-1832. We thank two reviewers for their insightful comments and suggestions which helped the presentation of this manuscript.

References

Aoki, S., Daerden, F., Viscardy, S., Thomas, I. R., Erwin, J. T., Robert, S., et al. (2021). Annual appearance of hydrogen chloride on Mars and a striking similarity with the water vapor vertical distribution observed by TGO/NOMAD. *Geophysical Research Letters*, *48*(11), e2021GL092506. https://doi.org/10.1029/2021GL092506

Atreya, S. K., Wong, A. S., Renno, N. O., Farrell, W. M., Delory, G. T., Sentman, D. D., et al. (2006). Oxidant enhancement in Martian dust devils and storms: Implications for life and habitability. *Astrobiology*, *6*(3), 439–450. https://doi.org/10.1089/ast.2006.6.439

Bak, E. N., Zafirov, K., Merrison, J. P., Jensen, S. J. K., Nørnberg, P., Gunnlaugsson, H. P., & Finster, K. (2017). Production of reactive oxygen species from abraded silicates. Implications for the reactivity of the Martian soil. *Earth and Planetary Science Letters*, *473*, 113–121. https://doi.org/10.1016/j.epsl.2017.06.008

Bandfield, J. L., Glotch, T. D., & Christensen, P. R. (2003). Spectroscopic identification of carbonate minerals in the Martian dust. *Science*, *301*(5636), 1084–1087. https://doi.org/10.1126/science.1088054

Boynton, W. V., Ming, D. W., Kounaves, S. P., Young, M. M., S., M. M., Arvidson, R. E., et al. (2009). Evidence for calcium carbonate at the Mars Phoenix landing site. *Science*, *325*(5936), 61–64. https://doi.org/10.1126/science.1172768

Carrier, B. L., & Kounaves, S. P. (2015). The origins of perchlorate in the Martian soil. *Geophysical Research Letters*, *42*(10), 3739–3745. https://doi.org/10.1002/2015GL064290

Catling, D. C., Claire, M. W., Zahnle, K. J., Quinn, R. C., Clark, B. C., Hecht, M. H., & Kounaves, S. (2010). Atmospheric origins of perchlorate on Mars and in the Atacama. *Journal of Geophysical Research*, *115*, E00E11. https://doi.org/10.1029/2009JE003425

Christensen, P. R., Wyatt, M. B., Glotch, T. D., Rogers, A. D., Anwar, S., Arvidson, R. E., et al. (2004). Mineralogy at Meridiani Planum from the mini-TES experiment on the opportunity rover. *Science*, *306*(5702), 1733–1739. https://doi.org/10.1126/science.1104909

Das, E., Glotch, T. D., Edwards, C. S., Ye, C., & Milliken, R. E. (2022). Hapke-based laboratory and remote determination of Martian chloride salt abundances. In *53rd lunar and planetary science conference*. LPI. Abstract 1480.

Delory, G. T., Farrell, W. M., Atreya, S. K., Renno, N. O., Wong, A. S., Cummer, S. A., et al. (2006). Oxidant enhancement in Martian dust devils and storms: Storm electric fields and electron dissociative attachment. *Astrobiology*, *6*(3), 451–462. https://doi.org/10.1089/ast.2006.6.451

Farrell, W. M., Desch, M. D., Kaiser, M. L., Houser, J., Landis, G. A., & Wilt, D. M. (2000). Radio and optical detection of Martian dust storm discharges. *Acta Astronautica*, *46*(1), 25–36. https://doi.org/10.1016/s0094-5765(99)00182-4

Farrell, W. M., McLain, J. L., Collier, M. R., Keller, J. W., Jackson, T. J., & Delory, G. T. (2015). Is the electron avalanche in a Martian dust devil self-quenching? *Icarus*, *254*, 333–337. https://doi.org/10.1016/j.icarus.2015.04.003

Frantz, J. D. (1998). Raman spectra of potassium carbonate and bicarbonate aqueous fluids at elevated temperatures and pressures: Comparison with theoretical simulations. *Chemical Geology*, *152*(3–4), 211–225. https://doi.org/10.1016/s0009-2541(98)00058-8

Glotch, T. D., Bandfield, J. L., Wolff, M. J., Arnold, J. A., & Che, C. (2016). Constraints on the composition and particle size of chloride salt-bearing deposits on Mars. *Journal of Geophysical Research: Planets*, *121*(3), 454–471. https://doi.org/10.1002/2015JE004921

Gure, A. J., Sorenson, T., Dewey, J. C., Kraus, T., Eggleston, C. M., & Parkinson, B. A. (2019). Photostationary state in photoelectrochemical generation of perchlorate: Relevance to Mars. *ACS Earth and Space Chemistry*, *3*(10), 2171–2174. https://doi.org/10.1021/acsearthspacechem

Harrison, R. G., BarthEsposito, E. F., Merrison, J., Montmessin, F., Aplin, K. L., Borlina, C., et al. (2016). Applications of electrified dust and dust devil electrodynamics to Martian atmospheric electricity. *Space Science Reviews*, *203*(1–4), 299–345. https://doi.org/10.1007/s11214-016-0241-8

Hecht, M. H., Kounaves, S. P., Quinn, R. C., West, S. J., Young, S. M. M., Ming, D. W., et al. (2009). Detection of perchlorate and the soluble chemistry of Martian soil at the Phoenix lander site. *Science*, *325*(5936), 64–67. https://doi.org/10.1126/science.1172466

Hill, J. R. (2022). *Martian chloride salts in the thermal infrared*, PhD thesis. Arizona State University. Retrieved from https://www.proquest.com/docview/2672291841

Korablev, O., Olsen, K. S., Trokhimovskiy, A., Lefèvre, F., Montmessin, F., Fedorova, A. A., et al. (2021). Transient HCl in the atmosphere of Mars. *Science Advances*, *7*, eabe4386. https://doi.org/10.1126/sciadv.abe4386

Kounaves, S. P., Hecht, M. H., Kapit, J., Gospodinova, K., DeFlores, L., Quinn, R. C., et al. (2010). Wet chemistry experiments on the 2007 Phoenix Mars Scout Lander Mission: Data analysis and results. *Journal of Geophysical Research*, *115*, E00E10. https://doi.org/10.1029/2009JE003424

Lide, D. L. (2001). *CRC handbook of chemistry and physics* (82nd ed.). CRC Press.

Martínez-Pabello, P. U., Navarro-González, R., Walls, X., Pi-Puig, T., González-Chávez, J. L., de la Rosa, J. G., et al. (2019). Production of nitrates and perchlorates by laser ablation of sodium chloride in simulated Martian atmospheres. Implications for their formation by electric discharges in dust devils. *Life Sciences and Space Research*, *22*, 125–136. https://doi.org/10.1016/j.lssr.2019.02.007

Olsen, K. S., Trokhimovskiy, A., Montabone, L., Fedorova, A. A., Luginin, M., Lefèvre, F., et al. (2021). Seasonal reappearance of HCl in the atmosphere of Mars during the Mars year 35 dusty season. *Astronomy and Astrophysics*, *647*, A161. https://doi.org/10.1051/0004-6361/202140329

Osterloo, M. M., Anderson, F. S., Hamilton, V. E., & Hynek, B. M. (2010). Geologic context of proposed chloride-bearing materials on Mars. *Journal of Geophysical Research*, *115*(E10), E10012. https://doi.org/10.1029/2010JE003613

Osterloo, M. M., Hamilton, V. E., Bandfield, J. L., Glotch, T. D., Baldridge, A. M., Christensen, P. R., et al. (2008). Chloride-bearing materials in the southern highlands of Mars. *Science*, *319*(5870), 1651–1654. https://doi.org/10.1126/science.1150690

Schuttlefield, J., Sambur, J., Gelwick, M., Eggleston, C. M., & Parkinson, B. A. (2011). Photooxidation of chloride by oxide minerals: Implications for perchlorate on Mars. *Journal of the American Chemical Society*, *133*(44), 17521–17523. https://doi.org/10.1021/ja2064878

Shi, E. B., Wang, A., & Ling, Z. C. (2019). MIR, VNIR, NIR, and Raman spectra of magnesium chlorides with six hydration degrees: Implication for Mars and Europa. *Journal of Raman Spectroscopy*, *51*(9), 1589–1602. https://doi.org/10.1002/jrs.5700

Tennakone, K. (2016). Contact electrification of regolith particles and chloride electrolysis: Synthesis of perchlorates on Mars. *Astrobiology*, *16*(10), 811–816. https://doi.org/10.1089/ast.2015.1424

Wang, A., Yan, Y. C., Dyar, D., Houghton, J., Farrell, W. M., Jolliff, B. L., et al. (2020). Amorphization of S, Cl-salts by Martian dust activities. *Journal of Geophysical Research: Planets*, *125*(12), e2020JE006701. https://doi.org/10.1029/2020JE006701

Wang, A., Yan, Y. C., Houghton, J., Jolliff, B. L., Jackson, A., Sturchio, N., et al. (2022). Martian carbonates generated by atmosphere-surface interaction. In *In 53rd lunar and planetary science conference*.

Wang, A., Yan, Y. C., Jolliff, B. L., McLennan, S. M., Wang, K., Shi, E. B., & Farrell, W. M. (2020). Chlorine release from common chlorides by Martian dust activity. *Journal of Geophysical Research: Planets*, *125*(6), e2019JE006283. https://doi.org/10.1029/2019JE006283

Wang, H., & Richardson, M. I. (2015). The origin, evolution, and trajectory of large dust storms on Mars during Mars years 24–30 (1999–2011). *Icarus*, *251*, 112–127. https://doi.org/10.1016/j.icarus.2013.10.033

Wilson, E. H., Atreya, S. K., Kaiser, R. I., & Mahaffy, P. R. (2016). Perchlorate formation on Mars through surface radiolysis-initiated atmospheric chemistry: A potential mechanism. *Journal of Geophysical Research: Planets*, *121*(8), 1472–1487. https://doi.org/10.1002/2016JE005078

Wu, Z. C., Wang, A., Farrell, W. M., Yan, Y. C., Wang, K., Houghton, J., & Jackson, A. W. (2018). Forming perchlorates on Mars through plasma chemistry during dust events. *Earth and Planetary Science Letters*, *504*, 94–105. https://doi.org/10.1016/j.epsl.2018.08.040

Zhao, Y.-Y. S., McLennan, S. M., Jackson, W. A., & Karunatillake, S. (2018). Photochemical controls on chlorine and bromine geochemistry at the Martian surface. *Earth and Planetary Science Letters*, *497*, 102–112. https://doi.org/10.1016/j.epsl.2018.06.015

References From the Supporting Information

Cantor, B. A. (2007). MOC observations of the 2001 Mars planet-encircling dust storm. *Icarus*, *186*(1), 60–96. https://doi.org/10.1016/j.icarus.2006.08.019

Estrada, N. L., Anderson, T. A., Böhlke, J. K., Gu, B. H., Hatzinger, P. B., Mroczkowski, S. J., et al. (2021). Origin of the isotopic composition of natural perchlorate: Experimental results for the impact of reaction pathway and initial ClO_x reactant. *Geochemica Cosmochemica Acta*, *311*, 292–315. https://doi.org/10.1016/j.gca.2021.06.039

Fedorova, A. A., Montmessin, F., Korablev, O., Luginin, M., Trokhimovskiy, A., Belyaev, D. A., et al. (2020). Stormy water on Mars: The distribution and saturation of atmospheric water during the dusty season. *Science*, *367*(6475), 297–300. https://doi.org/10.1126/science.aay9522

Kounaves, S. P., Chaniotakis, N. A., Chevrier, V. F., Carrier, B. L., Folds, K. E., Hansen, V. M., et al. (2014). Identification of the per-chlorate parent salts at the Phoenix Mars landing site and possible implications. *Icarus*, *232*, 226–231. https://doi.org/10.1016/j.icarus.2014.01.016

Qi, H., Mooen, H., Meijer, H. A. J., Coplen, T. B., Aerts-Bijma, A. T., Reid, L., et al. (2021). USGS44, a new high-purity calcium carbonate reference material for $d^{13}C$ measurements. *Rapid Communications in Mass Spectrometry*, *35*, e9006. https://doi.org/10.1002/rcm.9006

Shirley, J. H. (2015). Solar System dynamics and global-scale dust storms on Mars. *Icarus*, *251*, 128–144. https://doi.org/10.1016/j.icarus.2014.09.038

Sobron, P., & Wang, A. (2011). A planetary environment and analysis chamber for combined in-situ spectroscopic measurements on selected materials under planetary relevant environments. *Journal of Raman Spectroscopy*, *43*(2), 212–227. https://doi.org/10.1002/jrs.3017

Yan, Y. C., Wang, A., & Wu, Z. C. (2017). A simulated electro-chemical reaction for the generation of oxidants in near-surface atmosphere and the Cl-1 to Cl+X phase transformation at Martian surface. In *48th LPSC*.